

Design Of A New Layered Composite Membrane Based On A Physical Copolymer (PSU / PEI / PPc) Supported By A Tri-Component Support (PA6 / Fiberglass / PA6). Application of Ultrafiltration Baths Based On Azoic and Antraquinonique Dyes.

Said. Benkhaya ^{a*} and Ahmed. EL harfi ^a

^aLaboratoire Agro-Resources, Organic Polymers and Process Engineering (LARPOGP)/Team Organic Chemistry and Polymer (ECOP). Faculty of Sciences University Ibn Tofail, B.P.133, 14000 Kénitra-Morocco.

Abstract

An asymmetric porous tri-component support coated with a thin hydrophilic layer and active physical copolymer (Polyetherimide, Polysulfone and filled Polypropylene by 80% TiO₂) noted (PEI / PSU / PP_c) was used to synthesize a new composite membrane tri-component collodion for ultrafiltration. The prepared membrane was characterized by scanning electron microscope (SEM) and the mechanical property by a tensile testing machine. The ultrafiltration process was used to treat a family of reactive dyes (blue 49 and orange 16) from synthetic aqueous solutions and for raw textile effluents supplied from the rinsing / padding baths of the textile industry. The flow and the selectivity of the membrane during are directly related to the thickness of the active film, the pore size and the molecular weight of the reactive dye. The color retention performance, the chemical oxygen demand (COD) and conductivity were evaluated to determine the separating performance of the membrane. The conductivity rate is > 67%, the high COD and the color retention is (> 86%) were obtained by this composite membrane vis-à-vis the two dyes investigated in an alkaline medium at the upstream and downstream of the membrane.

* Corresponding author:

Benkhaya01said@gmail.com.

Received xxNov 2016, Revised

xxDec 2016, Accepted

xxDec 2016

Keywords: Tri-component Collodion, layered composite membrane, Copo (polysulfone, polyetherimide, polypropylene loaded by 80% of TiO₂ noted (PSU/PEI /PP_c), Ultrafiltration, reactive dye (antraquinonique and azoic).

1. Introduction

The textile industry plays an important role in the global economy of our life. It consumes large quantities of water both for finishing, fixing dyes on the substrate, and generating large amounts of waste waters. [1] Thus, the discharged effluents are highly altered by dyes [2, 3], auxiliary chemicals [3, 4], dissolved solids, suspended elements [4, 5] and colloidal particles [6]. Each year, many sectors of the textile industry reject a large amount of wastewater containing synthetic dyes into rivers without treatment by producing more wastewaters [7, 8]. These are loaded with various non-biodegradable and harmful components for the [9] environment. To preserve the quality of water courses [10, 11] for aquatic life, pre-treatment and / or treatment of wastes are necessary for the protection of nature. Indeed, several processes for treating wastewaters of textile industries can be applied such as wastewater treatment stations (WWTPs). These industries apply several steps according to STEP employed norms. We notice that industries [12] of textile generally use the two-step lagoon techniques rather than the activated sludge or biological drive. Therefore, outgoing water is only clarified. Hence the necessity for a tertiary phase to enhance the purified water. It should be composed by physico-chemical methods such as the coagulation-flocculation method [13], adsorption [14] Oxidation [15], electro-chemistry [16] and optionally the membrane processes [17, 18]. The purpose of this work is to study the performance of a new asymmetric composite membrane tri-matrix components (PSU / PEI / PPc) in the field of ultrafiltration [19-20], using rejection as aqueous solutions, rinsing baths and textile padding. The dyes thus employed in the formulation of these baths are the blue suncion and the orange Sunzol.

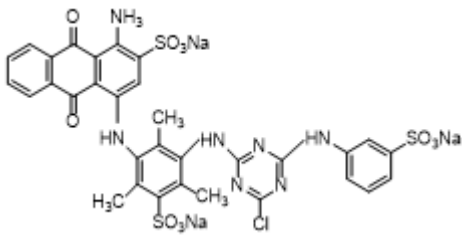
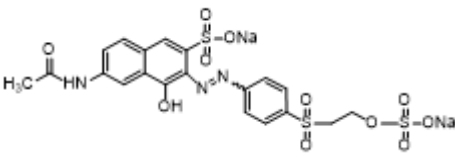
2. Materials and methods

The work was done in three steps: synthesis of a new asymmetric composite membrane of tri-component matrix (PSU / PEI / PPc), supported by an asymmetric porous technological support; microscopic characterizations and hydrodynamics of the optimized composite membrane; Ultrafiltration of rinsing / padding solutions of textile based on blue suncion and orange sunzol.

2.1. Characterisation of dyes

Table 1 shows the physicochemical characteristics of commercial dyes used in our study.

Table 1: Physicochemical characteristics of commercial dyes used in our study

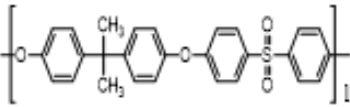
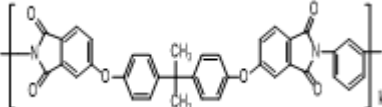
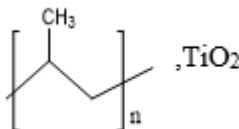
Features	Blue 49	Orange 16
Molecular structure		
Molecular mass	882.19g.mol ⁻¹	617.54g.mol ⁻¹
Empirical formula	C ₃₂ H ₂₃ ClN ₇ Na ₃ O ₁₁ S ₃	C ₂₀ H ₁₇ N ₃ Na ₂ O ₁₁ S ₃
Basic Structure	Anthraquinonic	Azoic
λ _{max} (nm)	595 nm	388 nm
Domain of Application	Textile	Textile

2.2. Structures of the membrane material components

2.2.1 Formulation of the active film by physical copolymer (PSU / PEI/PPc)

The table 2 shows the structure of each copolymer used in the development of laminated membrane.

Table 2: Structure of each copolymer used in the development of laminated membrane

Structures of membrane materials			
	PSU	PEI	PPc
Properties			
Physico-chemical	<ul style="list-style-type: none"> •Its color is yellow and transparent; •Good resistance to acids, bases, oils, grease and surfactants; •Good dimensional stability. 	<ul style="list-style-type: none"> •Density = 1.27 g / cm³; •low coefficient of linear thermic expansion; •Water absorption at 23 ° C is (1.25%). 	Unbound polypropylene <ul style="list-style-type: none"> •Low density (0.91 g / cm³); •Very good resistance to high temperatures; •Low water absorption at 23 °C (0.02%); •Good resistance to acids, alkalis, salt solutions, solvents, alcohols and water; •No resistance to acids, oxidizers, aromatic hydrocarbons and xylene.
Mechanical	<ul style="list-style-type: none"> •Good mechanical characteristics (rigidity, etc.). 	<ul style="list-style-type: none"> •Resistance to flow-strength to 50mm / min (105 MPa); •Elongation at flow-traction to 50 mm / minute (6 MPa); •Resistance to flexion to flow at 2 mm / min (160 MPa). 	<ul style="list-style-type: none"> •Tensile strength 21-37 N / mm².
Thermal	<ul style="list-style-type: none"> •Amorphous having a glass transition temperature between 180 and 190 ° C. 	<ul style="list-style-type: none"> •Deflection Temperature is (1.80 MPa A190 ° C); •Deflection Temperature is (0.45 MPa at 200 ° C). 	<ul style="list-style-type: none"> •Continuous use of temperature (-30 / + 100 ° C); •Melting point (180 ° C).
Electrical	<ul style="list-style-type: none"> •The PSU has good electrically insulating properties also called di-electric. 	<ul style="list-style-type: none"> •50 Hz di-electric constant is (2.9); •Dielectric Constance 1 MHz is (2.9). 	<ul style="list-style-type: none"> •Di-electric strength 80 KV / mm.

2.3. Molecular structures of the support

2.3.1. Polyamide 6

Polyamides also called nylon are technological macromolecular materials presenting good mechanical properties used in areas more and more varied such as automotive, electronics, tire reinforcements and textile industry...

2.3.1.1. Synthesis of PA6

The basic chemical reaction is a poly-condensation by the opening of the Precursor, cyclic amide caprolactam which leads to polyamide 6 (PA6), figure 1.

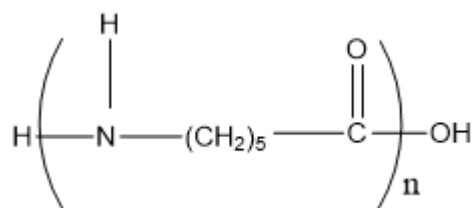


Figure 1: Chemical structure of PA6

2.3.1.2. Fiberglass

According to Figure 2, Glass fibers present the reinforcement of the composite material which usually provide the advantageous mechanical properties to the supported membrane.



Figure 2: Photograph of fiberglass

Table 3 regroups mass composition of the type of fiberglass E used in our study.

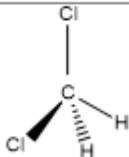
Table 3: Mass composition of the type of fiberglass E

Elements	Formula	Mass composition (%)
Silica	SiO ₂	53 à 56
Alumina	Al ₂ O ₃	12 à 16
Lime	CaO	21 à 24
Magnesia	MgO	21 à 24
Boron oxide	B ₂ O ₃	5 à 9
Fluorine	F	0 à 1
Sodium oxide	NaO ₂	≈ 1
Potassium oxide	K ₂ O	≈ 1
Zirconia oxide	ZrO ₂	-
Iron oxide	Fe ₂ O ₃	1
Titanium oxide	TiO ₂	1

2.4. Nature of solvents

Table 4 illustrates dichloromethane characteristics used as solvent in the collodion It is supplied by Sigma-Aldrich society.

Table 4: Dichloromethane characteristics used as solvent in the collodion

Solvent	Structure	Formula	Molar Mass	Density
Dichloromethane		CH_2Cl_2	84,93 g/mol	1,33 g/cm ³

2.5. Bath of Ultrasound

The ultrasonic bath (figure 3) accelerates the dissolution and spray fillers of polypropylene / TiO₂ by mechanical effects. The ultrasonic waves are generally between 20 and 400 kHz.



Figure 3: Ultrasonic bath

2.6. Implementation of the membrane

Technological support with a diameter of 2.5 cm was washed successively with distilled water to remove surface contaminants. The latter is then dried in an oven at 50 ° C for 15 min. The membrane was synthesized by a coating method as follows: In a solvent, the copolymer was sonicated for 30 minutes in an ultrasonic bath to ensure spraying the titanium dioxide particles in the membrane structure. The preparation thus obtained was then poured onto the upper face of the support. Then the collodion was spread by a thin stainless blade. The membrane is then placed in an oven for 30 minutes at 50 ° C.

2.7. Mounting the ultrafiltration cell

All experiments were performed in the laboratory using a cylindrical ultrafiltration cell of 36 cm³ (Figure 4) including a magnetic stirrer to homogenize the feeding solution and a porous aluminum support (Figure5).

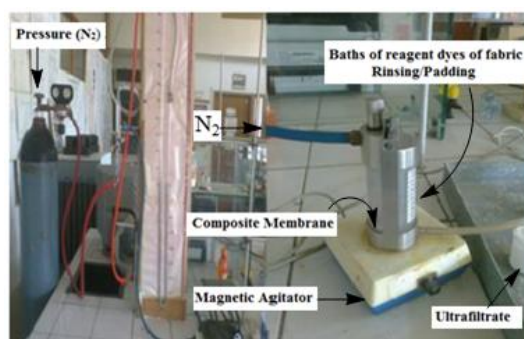


Figure 4: Photo of the ultrafiltration cell

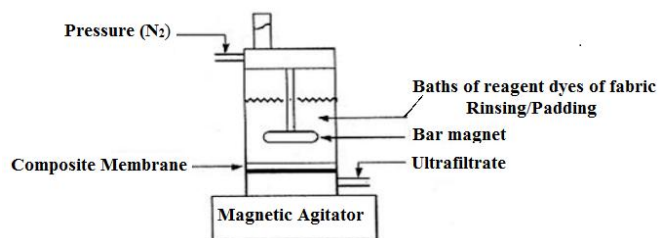


Figure 5: Figure of the ultrafiltration cell

The permeate rate was calculated by continuously measuring the volume of ultrafiltrate according to time and pressure successively during the filtration. Between each measurement, the system is cleaned with appropriate solutions and distilled water.

2.8. The UV-Visible Spectroscopy

The characterization of rinsing / padding baths of textile was made by the UV-visible spectrophotometry EVOLUTION 300 UV-VIS (Figure 6), at the maximum absorption wavelength.



Figure 6: Photo of UV-visible spectrophotometer

We subsequently determine the optical densities before and after the filtration, and therefore the discoloration rate (% TD) of the baths according to the following relationship [21]:

$$TD(\%) = \frac{DO_i - DO_f}{DO_i} \times 100$$

Where:

DO_i : is the optical density of bath before filtration;

DO_f : is the optical density of bath after filtration.

The Experience shows that for a little concentrated absorbent solution (textile dye), the absorbance A is proportional to the length of the vessel and to the concentration of C of the absorbing substance that reflects the law of Beer Lambert:

$$A = \epsilon_{\lambda_{max}} \cdot l \cdot C$$

Where:

A : absorbance; l : distance travelled by the light beam through the solution ($l = 1 \text{ cm}$);

C : concentration bath (mg / l or mol / l); $\epsilon_{\lambda_{max}}$: molar extinction coefficient of bath at a maximum wavelength (λ_{max}).

2.9. Fourier Transform Infrared Spectroscopy (FTIR)

The used IR spectrometer is a Fourier Transform Spectrometer (FTIR). The light beam passes through the sample to a thickness of a few micrometers. The analysis is performed between 4000 cm^{-1} and 800 cm^{-1} .

2.10. Nuclear magnetic resonance (NMR)

^1H NMR and ^{13}C analyzes were obtained using an apparatus of BRUKER AVANCE 300 MHz (Figure 7). The used solvent is CDCl_3 and chemical displacements are expressed in ppm.



Figure 7: Nuclear Spectrometer Magnetic Resonance "ADVANCE 300MHz of BRUKER"

2.11. Scanning electron Microscope SEM

The morphology of the membranes was performed by scanning electron microscope (SEM). This technique is based on the use of a beam of accelerated electrons by a fixed potential which excites the sample's surface. The interaction between the primary electron with the substance leads to the emission of secondary electrons, backscattered electrons, X-rays and Auger electrons.

2.12. Traction machine

The used apparatus is a tensile machine (Figure 8). This apparatus comprises a force sensor which translates the applied force into electric potential to a sample during its deformation.



Figure 8: Tensile testing machine

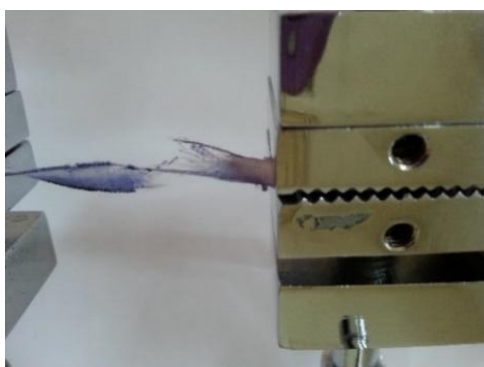


Figure 9: Tensile machine Jaws

The sample is attached to two jaws one of which is fixed and the other is mobile (Figure 9). The movable jaw is attached to a crosspiece through the force sensor. The crosshead moves on two screws at a predetermined speed through a gear system. During stretching, the force sensor transmits a signal proportional to the force imposed on the sample. The force sensors are only sensitive in a limited range of forces, but they are easily interchangeable.

2.13. Preparation of solutions of textile rinsing / padding bath

The two textile rinsing / padding baths were prepared according to the following protocol: The dissolution of 0.17 g of dye powder in a 250 ml flask containing distilled water. This mixture was heated for 30 min at a temperature of 80 ° C to ensure the complete dissolution of the dye. After cooling, the flask contents were poured into a 250 ml flask. Then an amount of 0.10 g of NaCl was added and supplemented with distilled water to the mark. The pH was adjusted to 10 with 5M sodium hydroxide and the prepared solutions were homogenized by magnetic stirrings. The concentration of dye and the NaCl concentration are respectively 6,8.10⁻⁴mol / l and 4, 2.10⁻² mol / l. Table 5 shows the key parameters characterizing the textile rinsing / padding solutions.

Table 5: Characteristics of textile solutions of rinsing / padding baths

Parametre	Unit	Orange Sunzol	Blue Suncion
Molecular weight	(g mol ⁻¹)	617.54	882
pH		10.13	10.46
Conductivity	(μS cm ⁻¹)	5600	7222
[dye]	(mol l ⁻¹)	6,8.10 ⁻⁴	6,8.10 ⁻⁴
DCO	(mol l ⁻¹)	512	414
[NaCl]	(mg l ⁻¹)	4,2.10 ⁻²	4,2.10 ⁻²

2.14. The analytical methods

The pH and conductivity were respectively determined by means of the pH meter and conductivity meter. The color retention, COD and salt were calculated by the following equation:

$$R = 100 * \left(1 - \frac{C_p}{C_a}\right)$$

C_p: the concentration of the permeate;

C_a: the power concentration.

3. Results and Discussions

The obtained active film composite membrane was characterized by proton and carbon-13 and Fourier Transform Infrared (FTIR). Spectra of the materials constituting the active membrane are given in Figures 10 and 11.

3.1. Microscopic characterization

3.1.1. NMR studies of the membrane {¹H} and {¹³C}

Figures 10 and 11 presents the characterization by spectroscopy the Nuclear Magnetic Resonance (NMR) of the synthesized membrane.

Fig 12 gives the infrared spectrum in Fourier transform (FTIR) macromolecular matrices used in the synthesis of the membrane.

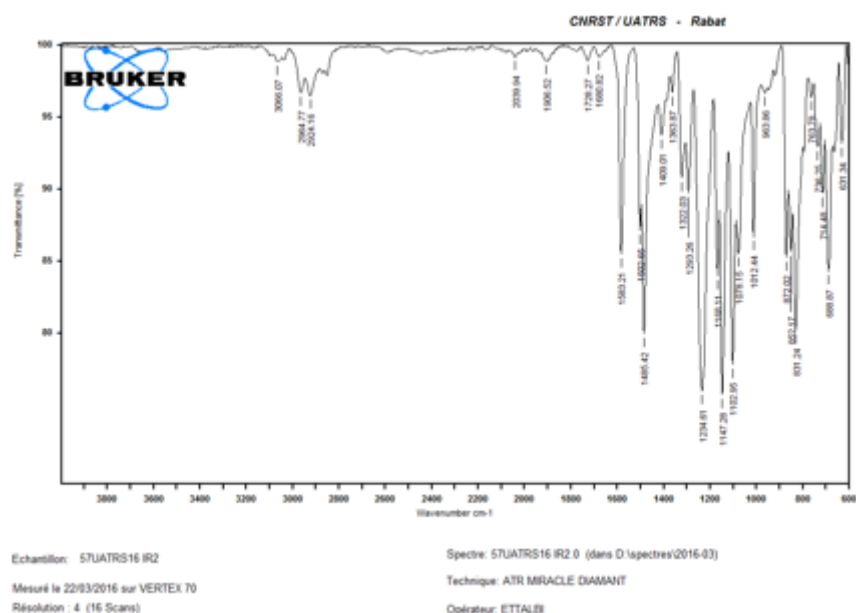


Figure 12: IR spectrum of the active layer

This spectrum shows the drain that characterizes the used copolymer (PSU / PEI / PPc) for synthesizing the active film of the laminated membrane. Table 6 regroups the different bands of infrared absorption IR (PSU / PEI / PPc)

Table 6: Different bands of infrared absorption IR (PSU / PEI / PPc)

Functional groups (Link)	Wave number in cm-1
Ph-O	Enter 1170 and 1300
C-H Aromatic	Enter 3000 and 3100
C-H	Of 2850 at 3000
C=C Aromatic	2 bands around 1600 and 1 band in 1500
C-OH	1300 at 1400
C=O	Enter 1630 and 1710
C-N	Enter 1020 and 1220
C-H the CH ₂	To 730
SO ₂	1380-1300
C-Cl	1175-650

3.2. Morphological characterization of the membrane by the SEM

The morphology of the optimization of the composite membrane has been illustrated with the SEM according to Figure 13.

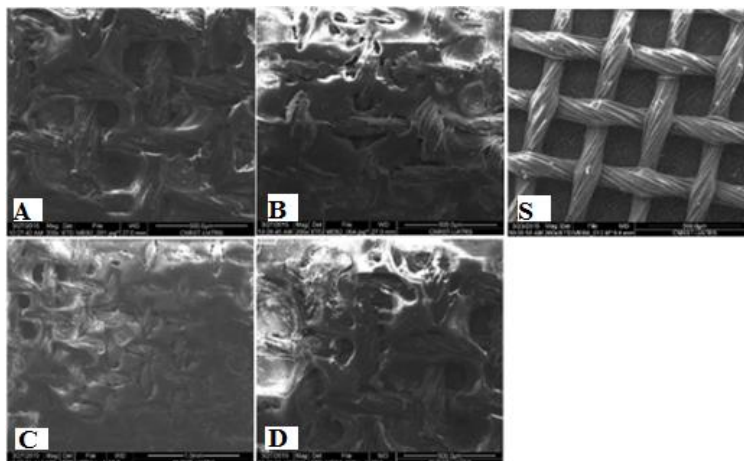


Figure 13: The morphology of the active membranes A, B, C, D and the support S

Indeed, the image S represents the support of the laminated membrane supporting the active phase while the pictures A, B, C and D represent the active surface of the composite membrane according to the mass composition of the physical copolymer (PSU / PEI / PPc) respectively (0.10 / 0.04 / 0.01); (0.15 / 0.05 / 0.02); (0.20 / 0.06 / 0.03); (0.25 / 0.07 / 0.04).

3.3. Mechanical properties of the membrane

Tensile tests obtained with the aid of the traction device are illustrated in Figure 14.

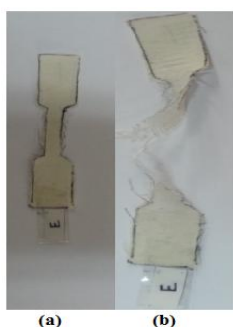


Figure 14: Specimen (a) and (b)

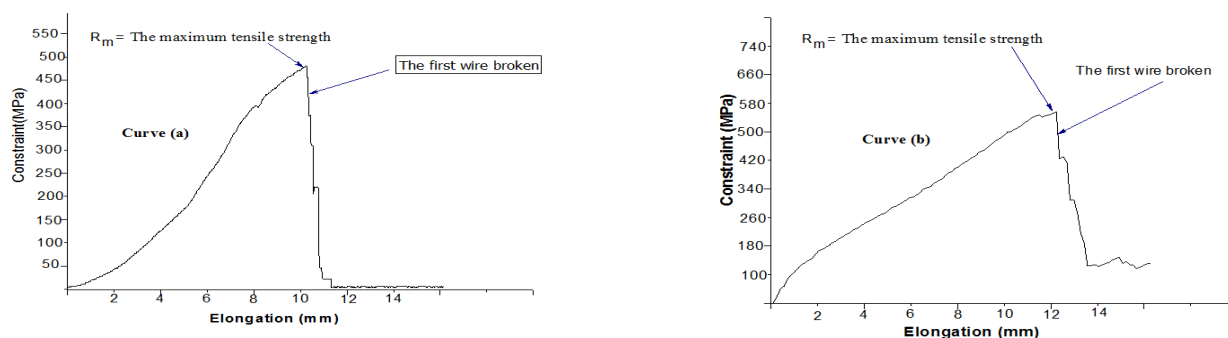


Figure 15: Tensile curves before (a) and after (b) coating

In fact, figures (a) and (b) show the resulting composite membranes respectively before and after the test of traction.

While the mechanical evaluation of the traction of the membrane support and that of the composite membrane are respectively illustrated by the curves (a) and (b) of Figure 15. Indeed, from the curves (a) and (b), we see an improvement of the composite membrane which is of $R_m = 575 \text{ MPa}$ relative to the support which is $R_m = 455 \text{ MPa}$.

3.4. Hydrodynamic caractérisation of the laminated membrane

3.4.1. Membrane permeability

Figures 16 and 17 represent the hydrodynamic characterization of the membrane depending on the pressure and time on the one hand and according to the mass composition of PSU, PEI and PPc on the other. It is given by the following relationship [22].

$$J_w = \frac{Q}{A \cdot \Delta t}$$

With:

J_w : ultra-pure water flow ($\text{l/h} \cdot \text{m}^2$); Q : the volume of water's permeate (l); A : effective membrane surface (m^2); Δt : The flow time in (h).

From Figure 16, the flow augments on the one hand according to the increase in transmembrane pressure between 3-6 bars and then remains constante with higher pressure of 6 bars. This is due to the saturation of the pores of the laminated membrane. On the other hand, this parameter is inversely proportional to the constituent mass percentage of the macromolecular matrix used in the synthesis of the membrane. According to Figure 17, we found that the flow du dominates during the membrane filtration according to the increase in time.

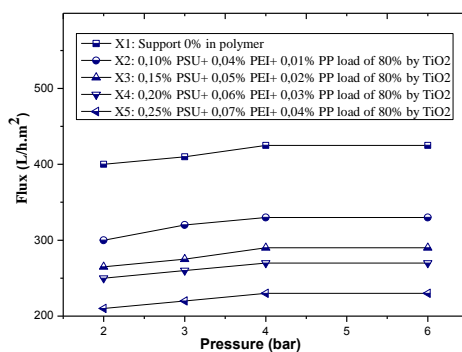


Figure 16: Flow rate according to the pressure

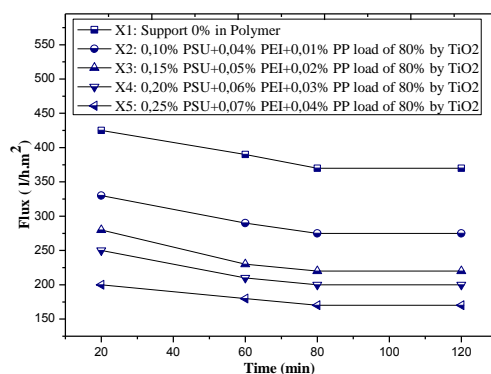


Figure 17: Flow rate according to the time

3.4.2. The selectivity of the membrane

Figure 18 below shows the selectivity of the membrane according to different molar masses of dextran.

To measure the selectivity of the laminated composite membranes, we calculated for each membrane the retention (%) R) of different dextrans solutions having molecular weight (g / mol): 500; 1000; 4000 and 8000 in a successive manner by subtracting the measurements of refractive index by a refractometer according to the following relationship [23]:

$$R(\%) = \frac{(n_i - n_{H_2O}) - (n_p - n_{H_2O})}{(n_i - n_{H_2O})} \times 100$$

With:

n_{H_2O} : Refractive index of the distilled water used; n_i : Refractive index of the dextran solution; n_p : Refractive index of the ultrafiltered solution of dextran.

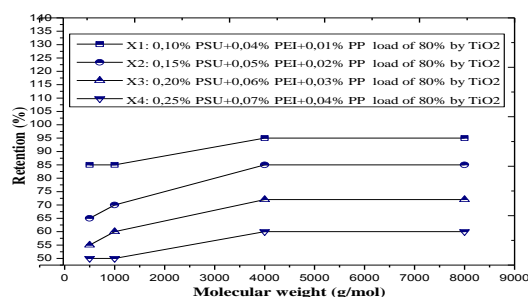


Figure 18: Dextran retention curves by composite membranes are obtained by mixtures of different masses PSU, PEI and PPc

From this figure, it is shown that the increase of the concentration of the constituent macro-molecular matrix used in the synthesis of membrane provokes an increase of aqueous solutions' selectivity of dextran of molecular weights between 500 and 4000 g / mol, then remains constant.

3.5. State of ultrafiltration in the treatment of rinsing / padding bath of textile

3.5.1. Bath retention rate

Figures 19 and f 20 below illustrate the color retention, COD and conductivity of the Rinsing / padding bath of textile after the ultrafiltration process.

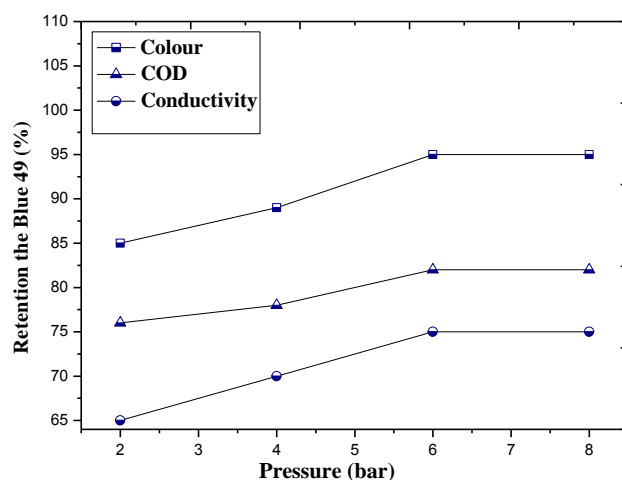


Figure 19: Retention rates depending on the transmembrane pressure by the membrane mass collodion 0.10 % PSU + 0.04% PEI + 0.01% PPc

According to the figures, we observed a strong color rate which was retained, a good retention of COD and a better conductivity rate for both rinsing / padding solutions of textile with transmembrane pressure upper to 6 bars. The

negatively charged membrane may increase the electrostatic repulsion of the investigated dyes which are characterized by anionic groups (sulfonic) that readily interact with the negative charge of the synthesized membrane. Which could justify the high retention of color and enhancing the retention of the salt which affects the conductivity retention ratio. Chemical forms, the number of active groups and the stability of a negative charge of the dye could give the different affinities of the membrane surface vis-a-vis these studied reactive dyes.

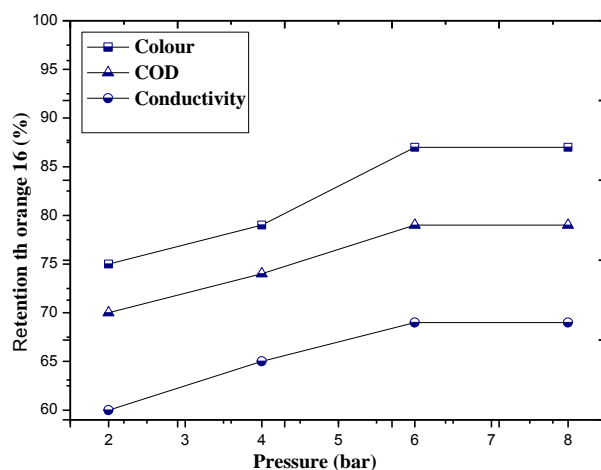


Figure 20: Retention rates depending on the transmembrane pressure by the membrane mass collodion 0.10 PSU% + 0.04 PEI % + 0.01% PPc

3.5.2. Chemical cleaning

Like all membrane processes, clogging is a major problem that must be solved. It is of multiple origins. It depends on the accumulation of dye molecules on the surface of the membrane. This accumulation acts as concentration polarization. [24] It is known as a factor that leads to increased fouling of the membrane attributed to the blockage of pores by initial formations [25, 26]. It must be removed by chemical cleaning which comprises the circulation of distilled water in the system for 40 min, followed by a basic cleaning with a sodium hydroxide solution (5 mol l^{-1}) at $\text{pH} = 11$ for 20 min. the installation is again rinsed with distilled water for 40 min. The steps of the cleaning process were followed without applying any pressure which could initiate the clogging of the membrane. After that, the permeability of the membrane was re-evaluated in order to check the status of membrane fouling.

4. Conclusion

We synthesized a laminated composite ultrafiltration membrane on a tri-component support (PA6 / fiberglass / PA6) coated by a physical copolymer (PSU / PEI / PPc).

The spectral characteristics of the active film were confirmed by NMR (^1H , ^{13}C) and FTIR while the porous structure was confirmed by the SEM. The mechanical properties prove to be interesting.

- The separating performance of the membrane was evaluated by the retention of color, the COD and the conductivity for ultrafiltrating two rinsing / padding bath solutions of textile summing up like this:
- A strong color retention ($> 86\%$), a better retention of COD ($> 76\%$) and a conductivity of ($> 67\%$) were obtained for the rinsing / padding bath solutions of textile to determine the separating performance of the composite membrane.
- We see an improvement of the composite membrane which is of $R_m = 575 \text{ MPa}$ relative to the support which is $R_m = 455 \text{ MPa}$.

- The UF process is an effective method for reducing the conductivity, the COD and the color retention in the textile effluents.

References

- [1] Ü. Tezcan Ün, S. Uur, A.S. Koparal, Ü. Bakr Öütveren, *Purif. Technol.* 52 (2006) 136-141.
- [2] S.P. PETROV., P.A. STOYCHEV. *Desalination.* (2003) 154, 247–252.
- [3] M. MARCUCCI., G. NOSENZO , G. CAPANELLI., I. CIABATTI., D. CORRIERI , G. GIARDELLI. *Desalination.* (2001) 138, 75–82.
- [4] A. Mittal, I. Mittal, A. Malviya, V. K. Gupta, *Colloid Interface Sci.* (2009), 340, 16-26.
- [5] A. S. Ozcan and A. J. Ozcan, *Colloid Interf. Sci.* (2004) 276, 39–46.
- [6] M. Bayramoglu, M. Kobya, O.T. Can, M. Sozbir. *Purif. Technol.* 37 (2004) 117–125.
- [7] J.M. Gozálvéz-Zafrilla, D. Sanz-Escribano, J. Lora-García, M.C. León Hidalgo, Nanofiltration of secondary effluent for wastewater reuse in the textile industry, *Des* 222 (2008) 272–279.
- [8] N. Zaghbani, A. Hafiane, M. Dhahbi. *J. Hazard. Mater.* 168 (2009) 1417–1421.
- [9] M. Saquib, M. Muncer. *Dyes and Pigments* . (2003) 56:37e 49.
- [10] E. Forgacs, T. Cserhati, G. Oros. A review, *Environ. Int.* 30 (2004) 953–971.
- [11] U. Rott, R. Minke. *Water Sci. Technol.* 40 (1999) 137–144.
- [12] C. Fersi, L. Gzara and M. Dhahbi. *Desalination*, 185 (2005) 1825–1835.
- [13] M. Franceschi, A. Girou, A. M. Carro-Diaz, M. T. Maurette, E. P. Costes. *Wat. Resear.* 36 (2002) 3561-3572.
- [14] S. Dawood, T. K. Sen, *Water Res.* (2012) 46, 1933-1945
- [15] G. Reynolds, N. Graham, R. Perry, R. G.. A.Rice, Review,” *Ozone Sci. Eng.* (1989) 11, 339-382.
- [16] Fan, L., Zhou, T., Yang, W., Chen, G., Yang, F. *Dyes Pigments.* (2008) 76, 440-446.
- [17] G. Klomfas and K. Konieczny . *Desalination*, 163 (2004) 311–322.
- [18] S. Srisurichan, R. Jiratananon and A.G. Fane, *J. Membr. Sci.*, 277 (2006) 186–194.
- [19] S. Benkhaya and A. El Harfi. *IJIAS.* 10 (2015) 285-294.
- [20] Y. He, G. Li, H. Wang, Z. Jiang, J. Zhao, H. Su, Q. Huang, *Chem. Eng.* 40 (2009) 289–295.
- [21] M. Rafik, A. Mas, A. El Harfi, F. Schue. *Eur. Polym. J.* 33 (5) (1997) 641-648.
- [22] B. Chakrabarty., A.K. Ghoshal, M.K, J. Purkait. *Membr. Sci.* 315 (2008) 36-47.
- [23] M. Rafik, A. Mas, A. El Harfi, F. Schue., *Eur. Polym. J.* 33 (5) (1997) 679-690.
- [24] R.C. Binning, R. J. Lee, J. F. Jennings, E. C. Martin., *Indust. Eng. Chem.* 53(1983) 45-50.
- [25] A. Broeckmann, J. Busch, T. Wintgens and W. Marquardt. *Desalination*, 189 (2006) 97–109.
- [26] L. Shu, A. Fane, T. Waite, M. Pailthorpe and P. Bliss, *World Filtration Congress, London* (2006) 647–650.